Nanotechnology **19** (2008) 125703 (7pp) doi:10.1088/0957-4484/19/12/125703

Measurement of metal/carbon nanotube contact resistance by adjusting contact length using laser ablation

Chun Lan[1,2], Pornsak Srisungsitthisunti[1,3], Placidus B Amama[1], Timothy S Fisher[1,3], Xianfan Xu[1,3] and Ronald G Reifenberger[1,2]

[1] Birck Nanotechnology Center, Purdue University, West Lafayette, IN 47907, USA
[2] Department of Physics, Purdue University, West Lafayette, IN 47907, USA
[3] School of Mechanical Engineering, Purdue University, West Lafayette, IN 47907, USA

E-mail: lan0@physics.purdue.edu

Received 2 January 2008, in final form 18 January 2008
Published 21 February 2008
Online at stacks.iop.org/Nano/19/125703

Abstract
A technique of measuring contact resistance between an individual nanotube and a deposited metallic film is described. Using laser ablation to sequentially shorten the contact length between a nanotube and the evaporated metallic film, the linear resistivity of the nanotube as well as the specific contact resistivity between the nanotube and metallic film can be determined. This technique can be generally used to measure the specific contact resistance that develops between a metallic film and a variety of different nanowires and nanotubes.

(Some figures in this article are in colour only in the electronic version)

1. Introduction

A seminal problem in the development of electronics at the nanometer length scale is a fundamental determination of the factors influencing the contact resistance between a thin metal film and a nanowire. Three factors contributing to contact resistance are (i) constriction of current flow due to the nanoscale geometry, (ii) the local chemistry that develops between the contact surfaces, and (iii) the alignment between the Fermi levels of the nanowire and the thin metallic film. The constriction of current can be described by an effective contact area which is determined by the local atomic structure between the metallic film and the nanowire. As the effective contact area increases, e.g. by thermal annealing, the contact resistance is expected to decrease. The local chemistry near the contact may contribute to the formation of oxides which produces a tunnel barrier. If no significant tunnel barrier forms, an ohmic contact of low resistance is expected if the Fermi level of the nanowire is aligned with the Fermi level of the metallic contact. All of these quantities are difficult to control. A systematic approach that allows an accurate measure of contact resistance and identifies the contributing factors has important applications in optimizing the integration of nanowire-based devices into circuits.

Because of their promise for advanced nanoelectronic applications, it is not surprising that the formation of reliable, low resistance contacts to carbon nanotubes (CNTs) have been discussed in the literature. For example, a number of theoretical discussions elucidating electrical contacts to CNTs have appeared [1–7]. In addition, experimental measurements of the contact resistance to CNTs have been published [8–11]. From this prior work, it seems clear that the contact resistance to a CNT can be significantly altered by many factors. A variation of contact resistance with the composition of the contacting metal film has been established [10], and Pd [12, 13] and Rh [14] thin films seem to offer clear advantages. Experimental studies to lower the resistance of existing contacts to single-wall carbon nanotubes (SWCNTs) indicate that the use of rapid thermal annealing [15], electrodeposited Au [16], and current-induced Joule heating techniques [17] all have beneficial effects.

While SWCNTs make attractive nanowires because of their nanometer diameter, multi-wall carbon nanotubes (MWCNTs) have additional advantages because they offer parallel conduction paths and exhibit high current carrying capabilities. Studies focused on lowering the contact resistance to MWCNTs have been reported utilizing electron beam exposure [18], electron beam soldering via the decomposition

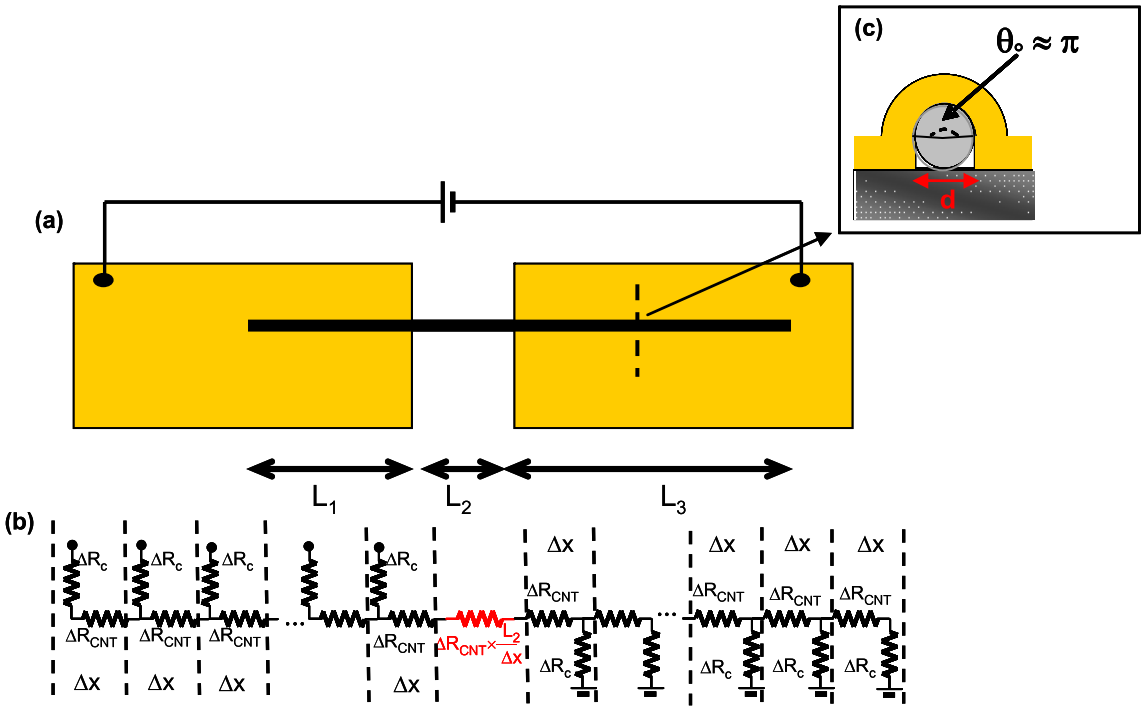

Figure 1. (a) A schematic diagram of a buried CNT contacted on either side by two contact pads comprised of a deposited thin film. The CNT is contacted by the thin film over lengths denoted as L_1 and L_3. The CNT bridges the two contacts across a center gap of width L_2. (b) A transmission line model that allows an estimate of the contact resistance. The contact resistance is modeled as a sequence of resistors of value ΔR_c that tie into the CNT along its entire length. (c) A cross-sectional schematic diagram of the contact.

of organometallic vapors [19], and current flow through Ti/Au electrodes [20]. A statistical study involving ∼20 MWCNTs suggests that the contact resistance scales inversely with contact length [21].

During the course of the above studies, two experimental techniques have been predominantly employed to measure the contact resistance to CNTs. A standard approach requiring high resolution lithography relies on a four-point probe technique [9, 18, 22]. Estimates of contact resistance have also been derived from a variety of atomic force microscope (AFM) techniques [7, 23–29].

In spite of the published work on CNTs, a clear understanding of the roles played by contact length, nanowire dimensions, and the contact metal still remains elusive. In some instances, seemingly contradictory results have been published. The difficulty may well be that individual CNTs possess significantly different defect structures (based on growth or processing conditions) which in turn significantly influence the contact resistance. Since the formation of low resistance contacts is required for the continued development of nanoelectronics, additional innovative techniques capable of systematically measuring the contact resistance between a wide variety of metal films and nanowires are highly desirable.

In this paper, we describe a method to simultaneously determine both the contact resistance and MWCNT resistance. Using a geometrical model of the contact area, the specific contact resistivity is determined, thereby allowing quantitative estimates for optimal contact pad dimensions once the diameter of a nanowire is specified. In what follows, we report on the results of our initial studies which use MWCNTs to validate the technique we have developed. By using a pulsed femtosecond laser to sequentially cut off sections of a MWCNT covered by a thin deposited metallic film, we show that both the resistance per unit length of a nanowire as well as the specific contact resistance between a given nanowire and a metallic film can be determined.

2. Theoretical model

We first describe a transmission line model for calculating the resistance of a MWCNT contacted by a metallic film. A similar model applied to semiconducting nanowires has been described elsewhere [30]. The elements of the model are given in figure 1(a) where we show a schematic diagram of a CNT covered at both ends by a deposited conducting film. Lengths L_1 and L_3 of the MWCNT make intimate contact to the metal film, while a length L_2 of the CNT bridges the gap between the two contact pads. As shown in the diagram, a bias voltage V is applied between the two contact pads. The total resistance of this structure can be obtained from the slope of I–V data near zero-bias.

The resistance of the CNT, R_{CNT}, is defined as:

$$R_{\mathrm{CNT}} = r_{\mathrm{CNT}} L_2, \tag{1}$$

where r_{CNT} (in kΩ μm^{-1}) reflects the quality of the CNT that is largely determined by CNT growth conditions. L_2 is the uncovered length of the CNT between the two metallic electrodes. The linear dependence of R_{CNT} on L_2 in equation (1) implies diffusive transport. In what follows, we

assume r_{CNT} is uniform along the length of the MWCNT. We also assume that r_{CNT} is not altered by the deposition of metal atoms. These assumptions suggest that our contact resistance model is more appropriate for larger diameter MWCNTs.

The specific contact resistance R_c is defined as

$$R_c = \frac{\rho_c}{A_c}, \tag{2}$$

where ρ_c is the specific contact resistivity, a quantity largely determined by the local chemistry between the surfaces of the metal film-CNT contact and the alignment between the Fermi levels of the CNT and the metallic film. A_c is the contact area.

For a CNT of outer diameter d contacted by a thin metal film, a transmission line model of the CNT/contact pads is shown in figure 1(b). The CNT is modeled as a number of series resistors each with length Δx. In this model, if the length of the CNT contact is L_1, then N_1 contacts are made to the CNT where $N_1 = L_1/\Delta x$. With these definitions, $\Delta R_{CNT} = r_{CNT}\Delta x$ while the incremental contact resistance over the length Δx can be written as $\Delta R_c = \frac{\rho_c}{A_c} = (\frac{2\rho_c}{d\theta_o})\frac{1}{\Delta x}$, where $A_c = [\frac{d}{2}\theta_o \Delta x]$ is the area of contact between the CNT and the metallic film over the length Δx and θ_o is the subtended angle of the metal film with the CNT as shown schematically in figure 1(c). Assuming $\theta_o \approx \pi$, we have $A_c \approx \pi t \frac{d}{2}\Delta x$. It follows that ΔR_c can then be written as:

$$\Delta R_c \approx \left(\frac{2\rho_c}{\pi d}\right)\frac{1}{\Delta x}. \tag{3}$$

For a particular CNT, if we assume the contacting electrodes form uniform contacts to both sides of the CNT, and if we ignore any variation in the outer diameter of the CNT over its length, then d and θ_o can be considered as constants.

To simplify the discussion, we define $r_c = \frac{2\rho_c}{d\theta_o} \approx \frac{2\rho_c}{d\pi}$ as the specific contact resistance for a unit length (in kΩ μm). With these definitions, we have $\Delta R_{CNT} = r_{CNT}\Delta x$ and $\Delta R_c = \frac{r_c}{\Delta x}$.

Let $R(x)$ equal the resistance of a CNT which is contacted by a metal film over a length x. Consider the change in resistance $\Delta R(x) = R(x + \Delta x) - R(x)$ when the contact length x is increased from x to $x + \Delta x$

$$R(x + \Delta x) = \Delta R_{CNT} + \frac{1}{\frac{1}{R(x)} + \frac{1}{\Delta R_c}}. \tag{4}$$

As $\Delta x \to 0$ (neglecting higher order terms), we have

$$\frac{dR(x)}{dx} = r_{CNT} - \frac{R^2(x)}{r_c}. \tag{5}$$

Upon integrating, we find a general expression for $R(x)$:

$$R(x) = \sqrt{r_{CNT}r_c}\left[\frac{1 + e^{-2\sqrt{\frac{r_{CNT}}{r_c}}x}}{1 - e^{-2\sqrt{\frac{r_{CNT}}{r_c}}x}}\right]$$
$$= \sqrt{r_{CNT}r_c}\coth\left(\sqrt{\frac{r_{CNT}}{r_c}}x\right). \tag{6}$$

In the limit when $x \to \infty$, the resistance R calculated from the above formula for the case of a MWCNT with outer diameter d is found to be $R(\infty) \approx \sqrt{r_{CNT}r_c} \approx \sqrt{\frac{2r_{CNT}\rho_c}{\pi d}}$, a quantity which depends on geometry and the intrinsic parameters only.

Returning to the geometry sketched in figure 1(a), we can see that the total resistance from a two-terminal measurement will be given by

$$R = \sqrt{r_{CNT}r_c}\coth\left(\sqrt{\frac{r_{CNT}}{r_c}}L_3\right) + r_{CNT}L_2$$
$$+ \sqrt{r_{CNT}r_c}\coth\left(\sqrt{\frac{r_{CNT}}{r_c}}L_1\right). \tag{7}$$

If the length of the right contact pad is shortened to have a length x, then the total resistance R will be given by

$$R(x) = \sqrt{r_{CNT}r_c}\coth\left(\sqrt{\frac{r_{CNT}}{r_c}}x\right) + r_{CNT}L_2$$
$$+ \sqrt{r_{CNT}r_c}\coth\left(\sqrt{\frac{r_{CNT}}{r_c}}L_1\right). \tag{8}$$

It is clear that the total resistance must saturate when the contact length is large. This fact is recovered for a sufficiently long contact length by realizing that $\sqrt{r_{CNT}r_c}\coth(\sqrt{\frac{r_{CNT}}{r_c}}L_1) \approx \sqrt{r_{CNT}r_c}$ is an appropriate approximation. With this approximation, equation (8) can then be written as

$$R(x) \approx \sqrt{r_{CNT}r_c}\coth\left(\sqrt{\frac{r_{CNT}}{r_c}}x\right) + r_{CNT}L_2 + \sqrt{r_{CNT}r_c}. \tag{9}$$

Figure 2 illustrates the predictions of this model for different parameters as x is varied. The effect of varying r_c (r_c is controlled by the deposition conditions) is illustrated in figure 2(a) and shows how the variation in the total resistance is influenced by contact length for a fixed r_{CNT}. A larger value of r_c requires a longer contact length to produce a minimum contact resistance. The effect of varying r_{CNT} (r_{CNT} is controlled by nanowire growth conditions) is illustrated in figure 2(b) and shows how the variation in the total resistance is influenced by the contact length for fixed r_c. A smaller value of r_{CNT} requires a larger contact length to produce the minimum contact resistance. This analysis suggests that r_c and r_{CNT} can be estimated if R can be measured after sequentially shortening a CNT contacted by a thin metal film contact pad in a controlled way.

In the case of a MWCNT with sufficient long contact lengths on both ends, we have $x \to \infty$, and the total resistance can be written as

$$R = 2\sqrt{r_{CNT}r_c} + L_2 r_{CNT} = 2\sqrt{\frac{2r_{CNT}\rho_c}{\pi d}} + L_2 r_{CNT} \tag{10}$$

where $2\sqrt{r_{CNT}r_c}$ is the total contact resistance and $L_2 r_{CNT}$ is the MWCNT resistance between the two terminals.

We note that this model is generally applicable beyond the case of CNTs and can also be used for calculating the contact resistance between any nanowire and a metallic film as long as the current flow through a nanowire is accurately approximated by diffusive transport. For the case of ballistic conduction, the above analysis must be extended.

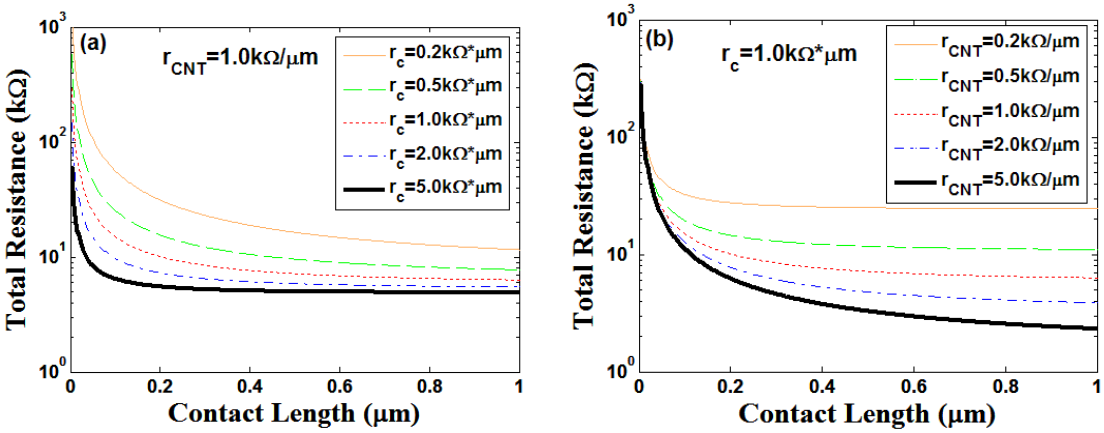

Figure 2. Representative plot of equation (9) to illustrate the effect of the parameters r_{CNT} and r_c on the predicted resistance as the contact length to a CNT is reduced. (a) The variation in the total resistance of a nanotube as one of the contacts is shortened. The CNT is assigned a representative linear resistivity of 1.0 kΩ μm^{-1}. As the contact length is shortened, the two-terminal resistance varies in a characteristic way according to the value of r_c, the specific contact resistance per unit length. (b) The predicted variation in the measured two-terminal resistance of different CNTs, each contacted by a metal film with a specific contact resistance per unit length of 1.0 kΩ μm. As the length of one of the contacts is shortened, the total resistance increases in a characteristic way according to the specified value of r_{CNT}, the linear resistivity of the nanotube. The calculations illustrate how the two-terminal resistance saturates as the contact length increases. The parameter L_2 (see figure 1(a)) used in these calculations is set to 4 μm.

3. Experimental details

The CNTs used in this study were chosen to be MWCNTs grown from Fe_2O_3 nanoparticles at 900 °C in a SEKI AX5200S microwave plasma-enhanced CVD (PECVD) reactor [31]. PECVD is known to introduce defects into the MWCNTs. The particular growth temperature of 900 °C was selected because prior studies have shown that this growth temperature produces the highest quality PECVD-grown CNTs [32]. These MWCNTs are plentiful and long enough ($\sim$30 μm) to allow a well-defined reduction in contact length using laser cutting. A detailed description of the PECVD system and the relevant CNT growth conditions has been reported elsewhere [33]. The catalyst fabrication process followed a procedure previously described [34].

Individual MWCNTs of $\sim$30 μm length, grown as described above, were randomly selected for this study. A sharp W tip was used to carefully extract an individual MWCNT from the as-grown MWCNT sample. After extraction, the MWCNT was transferred from the apex of the W tip onto a transparent substrate using a micromanipulator. The MWCNT was then masked by manipulating a tungsten wire using techniques previously developed [35]. After carefully positioning the tungsten wire shadow mask, Ti/Au electrodes were then thermally evaporated onto both ends of an individual MWCNT. From AFM measurements on a typical sample, we estimate the Ti film thickness to be $\approx$10 nm and the Au film thickness to be in the range of $\sim$50–100 nm. Similar sample preparation techniques were used for all samples studied.

A femtosecond laser system operating at 800 nm is used to cut a CNT sequentially. The femtosecond laser system produces pulses with 90 fs pulse duration, energies up to 1 mJ/pulse, and a pulse repetition rate of 1 kHz. A three-axis computer controlled positioning stage is used to move the sample with respect to the laser beam. The laser machining system is equipped with an in-line vision system which allows laser cutting at the desired location on the CNT. The laser pulses are focused onto the sample using a 100$\times$ microscope objective lens, which is able to produce a focused laser spot of about 1–2 μm on the target surface. We found that a laser pulse would occasionally dislodge the CNT from beneath the thin film, presumably due to a sudden heating of the substrate/film followed by a rapid relaxation of built-up strain in the CNT–thin film system. With care, we found that approximately 5–7 sequential cuts could be made without dislodging the CNT.

The experimental setup for acquiring I–V data of individual MWCNTs relies on a Kiethley 428 current amplifier interfaced to a laptop PC using Labview as described previously [32]. To avoid unwanted heating effects, $I(V)$ measurements were constrained to low bias conditions ($|V| \leqslant$ 0.1 V). Under these conditions, the measured $I(V)$ was found to be linear. The total resistance of the sample was reliably determined from the slope of a least squares fit to the $I(V)$ data. $I(V)$ data were acquired after each laser pulse shortened the MWCNT in a controlled way. After approximately 5 cuts were made, the sample was removed from the laser cutting station, and field-emission scanning electron microscope (FESEM) images were obtained to (i) better characterize the MWCNT, (ii) obtain the resulting contact length after each laser cut, and (iii) more accurately estimate the diameter of the MWCNT.

4. Results and discussion

Figure 3 shows a typical FESEM micrograph that illustrates the cumulative effect of a focused pulsed laser beam on a MWCNT contacted by an Ti/Au thin film. Initially, the laser was positioned away from the MWCNT and a number of calibrating cuts were made to optimize the laser power. These

Table 1. Summary of parameters from a least squares best fit to data for all the samples studied. The diameter of each MWCNT was estimated from FESEM micrographs.

Sample no.	Length between two terminals $L_2(\mu m)$	Diameter d (nm)	MWCNT resistivity r_{CNT} (kΩ μm^{-1})	Specific contact resistance per unit length r_c (kΩ μm)	Specific contact resistivity ρ_c ($\mu\Omega$ cm^2)
1	10.0 ± 0.1	225 ± 10	1.48 ± 0.02	1.3 ± 0.2	4.6 ± 0.7
2	10.0 ± 0.1	210 ± 10	0.51 ± 0.01	1.2 ± 0.2	4.0 ± 0.7
3	10.0 ± 0.1	130 ± 10	0.79 ± 0.02	4.2 ± 0.4	8.6 ± 1.0
4 (contact A)	4.0 ± 0.1	83 ± 10	0.33 ± 0.04	4.4 ± 0.8	6.0 ± 1.2
4 (contact B)	4.0 ± 0.1	83 ± 10	0.33 ± 0.01	5.3 ± 0.3	6.9 ± 0.9

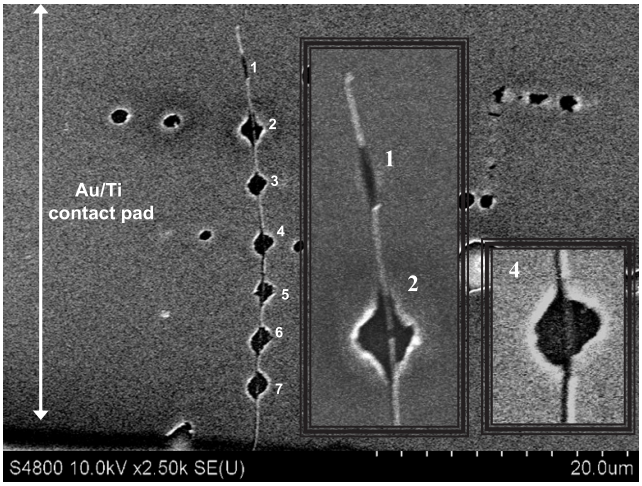

Figure 3. A representative micrograph showing an FESEM image of a MWCNT with evaporated contact pad after laser cutting. From this image, seven cuts have been made along the length of the MWCNT. The laser cuts made away from the MWCNT were performed to optimize the laser operating parameters. The edge of the gap separating the two thin film electrodes is just barely visible in the bottom left-hand edge of the micrograph. The figures in the inset show enlarged images of cuts 1, 2 and 4.

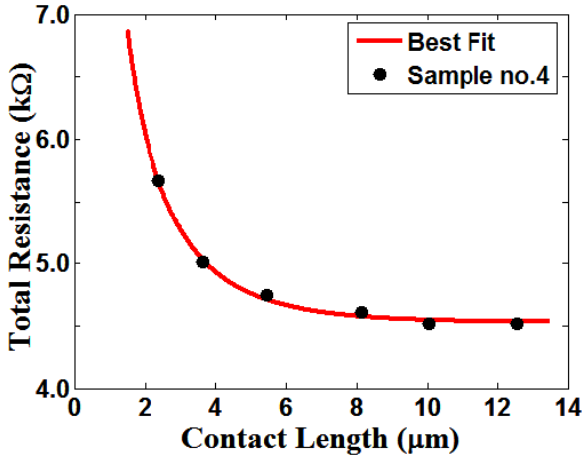

Figure 4. Resistance versus contact length for sample no. 4b. For this MWCNT, five cuts have been performed. From FESEM micrographs, the original contact length was measured to be $\sim$12.6 μm. The resistance plotted is the total resistance which includes both the contact resistance and the MWCNT resistance of the 4 μm section of the MWCNT. The solid line is the best fit to the data and gives parameters $r_{CNT} = (0.33 \pm 0.01)$ kΩ μm^{-1} and $r_c = (5.3 \pm 0.3)$ kΩ μm. The quoted uncertainties arise from the least squares fitting procedure.

calibration cuts appear as holes in the thin metallic film far from the MWCNT and are evident in figure 3. After the optimal conditions were achieved, the laser spot was positioned over the MWCNT, and a number of successive laser cuts were made. In some cases, although the Au film was well ablated by the laser pulse, the MWCNT was severed over a smaller region located in middle of the laser ablated film (see for example the enlarged inset of cut 2 in figure 3). FESEM images with higher resolution were taken as required to ensure the MWCNT was cut by the laser pulse. In figure 3, the laser cutting started from the top end of the micrograph and proceeded toward the gap between contact electrodes which is just visible at the bottom left-hand edge of the micrograph.

Figure 4 shows the resistance measured for a MWCNT (sample no. 4b) following each laser cut. Five cuts were made in this particular experiment. The original contact length was measured to be 12.6 ± 0.1 μm. Following the fifth cut, only $\sim$2.5 μm of the contact remained. The resistance was observed to continuously increase due to ever smaller contact length between the MWCNT sample and the Ti/Au electrode. The resistance plotted in figure 4 is the total resistance measured and includes the resistance from the 4 μm section of the MWCNT bridging the gap between the two separate Ti/Au electrodes.

To estimate the contact resistance, we apply the model derived above to the data plotted in figure 4. The least squares best fit to the data using equation (9) is shown by the solid curve in figure 4. For this sample, we found $r_c = 5.3 \pm 0.3$ kΩ μm and $r_{CNT} = 0.33 \pm 0.01$ kΩ μm^{-1}. The data agree with our model very well as evidenced by the small residual error between the experimental data and the best fit model curve.

A total of four different MWCNT samples were analyzed in this way, and the resulting fitting parameters are tabulated in table 1. In the fitting process, L_2 in equation (9) was set to be the length between the two terminals for each sample. The data labeled as sample no. 4a and sample no. 4b are from the same MWCNT. For this sample we performed sequential laser cuts on both of the contact electrodes. We note that the fitting parameters for the data from both sides of sample no. 4 agree very well. From table 1, we learn that r_{CNT} lies in the range of 0.33 to 1.48 kΩ μm^{-1}. This variation is most probably due to differences in the intrinsic defects in the MWCNTs. The measured r_c is in the range of 1.2–5.3 kΩ μm.

Table 2. Summary of the initial total resistance at zero-bias, the MWCNT resistance over length L_2, and the total contact resistance for each sample.

Sample no.	Initial total resistance (kΩ)	MWCNT resistance (kΩ)	Total contact resistance (kΩ)
1	17.56 ± 0.01	14.8 ± 0.20	2.77 ± 0.21
2	6.66 ± 0.01	5.1 ± 0.01	1.56 ± 0.13
3	11.73 ± 0.01	7.9 ± 0.20	3.64 ± 0.18
4 (contact A)	3.76 ± 0.01	1.32 ± 0.16	2.41 ± 0.26
4 (contact B)	4.51 ± 0.01	1.32 ± 0.05	3.28 ± 0.08

By using the values of r_{CNT} and r_c summarized in table 1, the total contact resistance ($2\sqrt{r_{CNT}r_c}$) and the MWCNT resistance between two the terminals ($L_2 r_{CNT}$) can be calculated. The summation of these two values matches the initial total resistance for all the measured samples as indicated in table 2[4].

An important feature of our model is that it provides an estimate of the specific contact resistivity ρ_c for the nanowire under study. In our case, the nanowire is a simple PECVD MWCNT grown at 900 °C with Ti/Au thin metal contacts. From the results given in table 1, an average value of $(6.0 \pm 1.8)\ \mu\Omega\ \text{cm}^2$ is found to characterize the thermally evaporated Ti/Au contact to PECVD-grown MWCNTs. This value is expected to be useful in estimating the contact resistance of other, similar CNT/contact structures fabricated by similar techniques. The utility of our experimental approach is that it provides a systematic method for characterizing a wide variety of different nanowires contacted by different metallic films.

Some factors other than geometry can potentially explain the observed variation in r_{CNT} and ρ_c. The MWCNTs in the present study have relatively large diameters in the range of 100 to 200 nm and contain many defect sites, which can cause variations in r_{CNT}. The thickness of Ti is another factor that is known to influence the contact resistance [10]. Carbon atoms contacting the outershell of a MWCNT tend to react with Ti to form a TiC layer with good conductivity [36]. Also, defects along the outer diameter of the MWCNTs may also cause the evaporated film to be chemically non-uniform.

In summary, we have developed a new technique for measuring the resistivity of a MWCNT and the specific contact resistivity of metallic Ti/Au thin films to an individual MWCNT. Using a pulsed femtosecond laser in conjunction with two-terminal $I(V)$ measurements, we were able to shorten the contact length systematically and to quantify the resulting change in resistance at the same time. From the data, both the MWCNT resistance and contact resistance can be obtained. A transmission line model that assumes diffusive transport conditions explains the data very well. The contact ablation technique described above is quite general and should be applicable to a wide range of other metal/nanostructure contacts.

[4] For sample no.4, we performed sequential laser cuts on both of the contact electrodes. The initial total resistance (3.76 kΩ) is comprised of the contact resistance from both contact A and contact B. After laser ablating contact A, the total measured resistance increased by ∼0.8 kΩ. Within the context of our model, this increase serves as an offset resistance which is added to the contact resistance after contact B was ablated.

Acknowledgments

We would like to thank Dr J Appenzeller for valuable discussions on the revised manuscript. We would also like to acknowledge the cheerful help of the staff of the Birck Nanotechnology Center at Purdue University.

References

[1] Xue Y and Datta S 1999 *Phys. Rev. Lett.* **83** 4844
[2] Rubio A, Sánchez-Portal D, Artacho E, Ordejón P and Soler J M 1999 *Phys. Rev. Lett.* **82** 3520
[3] Deng W-Q, Mastuda Y and Goddard W A III 2007 *J. Am. Chem. Soc.* **129** 9834
[4] Nardelli M B, Fattebert J-L and Bernholc J 2001 *Phys. Rev.* B **64** 245423
[5] Palacios J J, Pérez-Jiménez A J, Louis E, SanFabián E and Vergés J A 2003 *Phys. Rev. Lett.* **90** 106801
[6] Shan B and Cho K 2004 *Phys. Rev.* B **70** 233405
[7] Nemec N, Tománek D and Cuniberti G 2006 *Phys. Rev. Lett.* **96** 076802
[8] Ham M-H, Choi J-H, Hwang W, Park C, W-Y Lee and J-M Myoung 2006 *Nanotechnology* **17** 2203
[9] Stern E, Cheng G, Young M P and Reed M A 2006 *Appl. Phys. Lett.* **88** 053106
[10] Hwang J S, Ahn D, Hong S H, Kim H K, Hwang S W, Jeon B-H and Choi J-H 2004 *Appl. Phys. Lett.* **85** 1636
[11] Chen Z, Appenzeller J, Knoch J, Lin Y-m and Avouris P 2005 *Nano Lett.* **5** 1497
[12] Mann D, Javey A, Kong J, Wang Q and Dai H 2003 *Nano Lett.* **3** 1541
[13] Woo Y, Liebau M, Duesberg G S and Roth S 2004 *XVIII-th Int. Winterschool/Euroconference on Electronic Properties of Novel Materials* unpublished
[14] Kim W, Javey A, Tu R, Cao J, Wang Q and Dai H 2005 *Appl. Phys. Lett.* **87** 173101
[15] Lee J-O, Park C, Kim J-J, Kim J, Park J W and Yoo K-H 2000 *J. Phys. D: Appl. Phys.* **33** 1953
[16] Austin D W, Puretzky A A, Geohegan D B, Britt P F, Guillorn M A and Simpson M L 2002 *Chem. Phys. Lett.* **361** 525
[17] Woo Y, Duesberg G S and Roth S 2007 *Nanotechnology* **18** 095203
[18] Bachtold A, Henny M, Terrier C, Strunk C, Schönenberger C, Salvetat J-P, Bonard J-M and Forró L 1998 *Appl. Phys. Lett.* **73** 274
[19] Madsen D N, Mølhave K, Mateiu R, Rasmussen A M, Brorson M, Jacobsen C J H and Bøggild P 2003 *Nano Lett.* **3** 47
[20] Maki H, Suzuki M and Ishibashi K 2004 *Japan. J. Appl. Phys.* **43** 2027
[21] Wakaya F, Katayama K and Gamo K 2003 *Microelectron. Eng.* **67/68** 853
[22] Kanbara T, Takenobu T, Takahashi T, Iwasa Y, Tsukagoshi K, Aoyagi Y and Kataura H 2006 *Appl. Phys. Lett.* **88** 053118
[23] Dai H, Wong E W and Lieber C M 1996 *Science* **272** 523
[24] de Pablo P J, Gómez-Navarro C, Martínez M T, Benito A M, Maser M K, Colchero J, Gómez-Herrero J and Baró A M 2002 *Appl. Phys. Lett.* **80** 1462
[25] Schujman S B, Vajtai R and Ajayan P 2002 *Appl. Phys. Lett.* **81** 541
[26] Blanchet G B, Fincher C R, Lefenfeld M and Rogers J A 2004 *Appl. Phys. Lett.* **84** 296
[27] Yaish Y, Park J-Y, Rosenblatt S, Sazonova V, Brink M and McEuen P L 2004 *Phys. Rev. Lett.* **92** 046401
[28] Gómez-Navarro C, de Pablo P J, Gómez-Herrero J, Biel B, Garcia-Vidal F J, Rubio A and Flores F 2005 *Nat. Mater.* **4** 534

[29] Purewal M S, Hong B H, Ravi A, Chandra B, Hone J and Kim P 2007 *Phys. Rev. Lett.* **98** 186808
[30] Mohney S E, Wang Y, Cabassi M A, Lew K K, Dey S, Redwing J M and Mayer T S 2005 *Solid-State Electron.* **49** 227
[31] Meyyappan M, Delzeit L, Cassell A and Hash D 2003 *Plasma Sources Sci. Technol.* **12** 205
[32] Lan C, Amama P B, Fisher T S and Reifenberger R G 2007 *Appl. Phys. Lett.* **91** 093105
[33] Maschmann M R, Amama P B, Goyal A, Iqbal Z, Gat R and Fisher T S 2006 *Carbon* **44** 10
[34] Amama P B, Maschmann M R, Fisher T S and Sands T D 2006 *J. Chem. Phys.* B **110** 10636
[35] de Pablo P J, E Graugnard E, Walsh B, Andres R P, Datta S and Reifenberger R 1999 *Appl. Phys. Lett.* **74** 323
[36] Zhang Y, Ichihashi T, Landree E, Nihey F and Iijima S 1999 *Science* **285** 1719